CONF-9410254--9

UCRL-JC-121286
PREPRINT

Angular Biasing in Implicit Monte-Carlo

G. B. Zimmerman

Submittal to:
Code Developers Conference
Las Vegas, NV

October 25-28, 1994

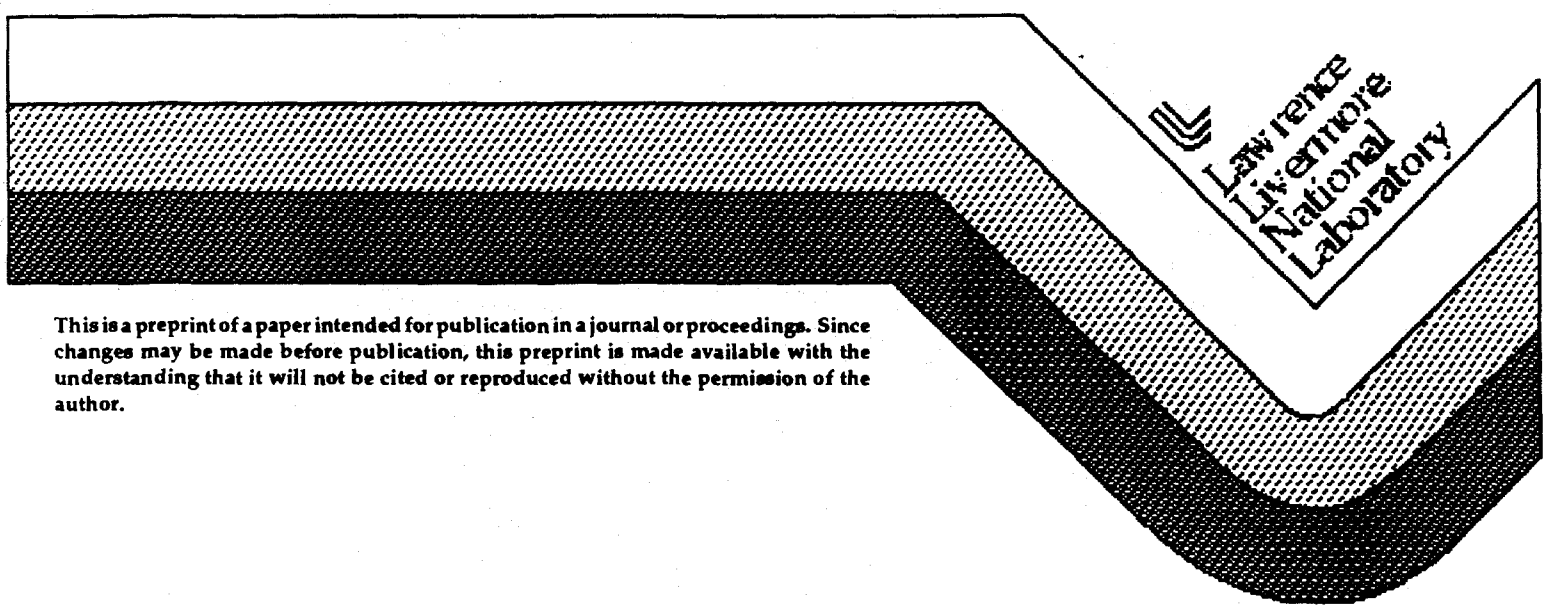

 85

DISCLAIMER

Portions of this document may be illegible in electronic image products. Images are produced from the best available original document.

Angular Biasing in Implicit Monte-Carlo

G. B. Zimmerman
Lawrence Livermore National Laboratory
October 20, 1994

Calculations of indirect drive Inertial Confinement Fusion target experiments require an integrated approach in which laser irradiation and radiation transport in the hohlraum are solved simultaneously with the symmetry, implosion and burn of the fuel capsule. The Implicit Monte-Carlo method has proved to be a valuable tool for the two dimensional radiation transport within the hohlraum, but the impact of statistical noise on the symmetric implosion of the small fuel capsule is difficult to overcome. We present an angular biasing technique in which an increased number of low weight photons are directed at the imploding capsule. For typical parameters this reduces the required computer time for an integrated calculation by a factor of 10. An additional factor of 5 can also be achieved by directing even smaller weight photons at the polar regions of the capsule where small mass zones are most sensitive to statistical noise.

I. Introduction

For decades the Implicit Monte-Carlo (IMC) method (Fleck and Cummings, 1971) has been used to simulate radiation transport in complicated multidimensional geometries. Its principal advantage over deterministic methods is the ease of implementation of all relevant physical effects, while its principal disadvantage is statistical noise.

Implicit Monte-Carlo has proved to be a valuable tool for the radiation transport in integrated hohlraum calculations of indirect drive Inertial Confinement Fusion target experiments. In these calculations laser deposition and radiation transport are solved simultaneous with the symmetry, implosion and burn of the fuel capsule, but the impact of statistical noise on the symmetric implosion of the small fuel capsule is difficult and expensive to overcome.

In Sec. II we present an angular biasing technique in which an increased number of low weight photons are directed at the imploding capsule. In Sec. III the method is further enhanced by directing even smaller weight photons at the polar regions of the capsule where small mass zones make the calculations most sensitive to statistical noise. Results of test calculations are presented in Sec. IV. We conclude with a discussion and summary in Sec. V.

II. Biasing toward a sphere

One of the most important aspects of IMC, the feature that makes it implicit, is the use of effective scatters as a replacement for a fraction of the absorption and emission. This stabilizes fluctuations in the material energy and guarantees positive material temperatures, but requires the use of numerical scattering even when the physical Compton scattering is negligible. Since scattering changes a photon's direction and since we are interested in controlling the weights of photons traveling in certain directions, it is clear that photon weights must be allowed to change during the scatter. This, of course, also requires that photons be statistically created and destroyed in the scatter.

The original IMC package assumed that exactly one photon came out of each scatter. This was an advantage in terms of simplicity (sizes of vector and census stacks could be precalculated), accuracy (exact energy conservation was possible) and speed (vectorization of the scattering process was straightforward). In order to implement angular biasing it was necessary to make changes in each of these areas: The sizes of particle storage areas were allowed to grow by using modern dynamic memory management methods. Exact energy conservation was replaced with statistical energy conservation which could then be used as an accuracy check. Vectorization of the scattering process was eliminated and placed at a low priority since most of the angular biased IMC calculations were to be done on workstations without vector processing units.

The methods used to sample the angularly biased photon distribution from volume and surface emission sources are detailed below. A method to handle Compton scattering has not yet been developed, but should be amenable to reasonably efficient rejection techniques. Currently one must turn off Compton scattering when using angular biasing.

Volume emission and effective scatters

In the IMC method both volume emission and effective scatters produce an isotropic angular photon distribution with a $\sigma_\nu B_\nu$ energy distribution, where σ_ν is the frequency dependent absorption cross-section and B_ν is the Planck function. Providing angular biasing of isotropic emission toward a spherical object, and even allowing for frequency biasing, is straightforward.

We establish a coordinate system in which the photon emission point is at the origin and the bias sphere center is on the z-axis. We take the photon importance to be $B(\mu)$, a function only of μ, the cosine of the photon direction relative to the z-axis. Sampling the photon direction consists of finding μ, where

$R = \int_{-1}^{\mu} B(x)\,dx / \int_{-1}^{1} B(x)\,dx$ and R is a uniform random variable on (0,1). The weight of the resulting photon is proportional to $1/B(\mu)$. In practice we have taken $B(\mu)$ to be a two step histogram corresponding to a spherical object with a core of one importance surrounded by a halo of another importance surrounded by the universe of unit importance.

Surface source emission

Emission from user defined surface sources has an angular distribution that depends on the angle between the photon direction and the surface normal. We have taken this to be a general power law,

$I(\vec{\Omega}) \propto (\vec{\Omega} \bullet \vec{n})^{\alpha}$, where α=1 for the usual cosine surface distribution. Providing for the angular biasing of such a distribution toward a spherical object is not straightforward because, in general, the direction of surface normal and the direction to the bias sphere are not the same. We have chosen to use a rejection scheme in which angularly biased isotropic photons are created just as for volume emission, then they are rejected if $\max(0, \vec{\Omega} \bullet \vec{n})^{\alpha} < R$. The efficiency of this rejection process is $1/(2\alpha+2)$, or 25% for the usual cosine distribution. This would be very inefficient as $\alpha \to \infty$, so surface normal emission is coded as a special case.

III. Biasing toward polar regions

In typical two dimensional axially symmetric Lagrange hydrodynamics calculations spherical objects are represented by equal angle zoning in the r-z plane. Zones near the poles have less mass than those near the equator and thus are more subject to statistical noise problems when irradiated with equal weight photons. The obvious solution is to enhance angular biasing in a way that directs more lower weight photons at the polar regions of the bias sphere.

For K equal angle zones in 90 degrees uniform irradiation of equal weight photons results in the polar zone receiving $\pi/4K$ as many photons as the equator zone. This is 1/25 for K=20. If one were to force the same number of photons to strike each angular zone -- keeping fixed the number hitting the equator -- it would take a total of only $\pi/2$ times as many photons. The potential gain then is $8K/\pi^2$ or 16 for K=20.

Unfortunately, this is risky business. Assigning photons weights based on the latitude of intersection with a bias sphere surface will only work well if the capsule is a hard sphere with infinite opacity inside and zero opacity outside. Density gradients on the capsule surface, frequency dependent opacities and the desire to specify a bias sphere as an envelope containing several disjoint objects all mean that there is a significant probability for photons to penetrate the bias sphere. In particular, Fig. 1 shows that photons entering the bias sphere near the equator can be absorbed near the polar region of a smaller sphere. This means that photon weights must be assigned based on the minimum polar angle of the trajectory within the bias sphere, not just the polar angle of the trajectory intersection with the bias sphere surface.

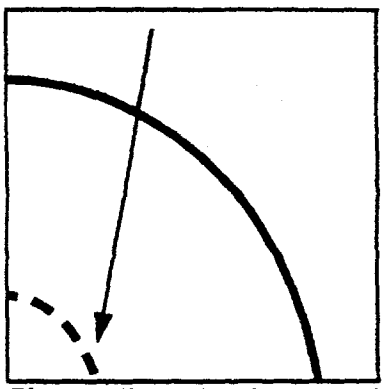

Figure 1. Photons directed at the equatorial region of the outer bias sphere may actually be absorbed near the polar regions of a smaller concentric sphere.

It would seem that assigning photons weights proportional to $\sin\theta_{min}$, where θ_{min} is the minimum polar angle of the trajectory within the bias sphere would automatically assure that each angular zone, whose mass is proportional to $\sin\theta$, would receive equal statistics. The problem is that the number of photons required to do this goes like $\int d\theta / \sin\theta$ and is logarithmically divergent. Also, if rejection techniques are used to establish the photon directions, then a lower limit on the photon weight must be established.

Fortunately, there is little advantage in achieving

photon weight reductions within the smallest polar zone, so placing a lower limit on $\sin\theta_{min}$ of about 1/K should not adversely affect the statistics. We will call this lower limit $1/P_{max}$ and evaluate its optimal value in test calculations. Using such a limit the total number of photons required -- leaving the number hitting the equator unchanged -- is no longer divergent, but is larger than the non-polar biased case by a factor of about $(1 + 2/\pi \bullet \log P_{max})$. The expected gain from polar biasing then is about $P_{max} / (1 + 2/\pi \bullet \log P_{max})$ where P_{max}~K. For P_{max}=20 this gain is 6.9, significantly less than the 16 possible for a hard sphere capsule, but still quite substantial.

Polar biasing is implemented entirely by rejection techniques. Using the previously described methods we sample photons uniformly toward the bias sphere with importance increased by a factor of P_{max}. For each photon we then evaluate θ_{min}, the minimum polar angle of the trajectory within the bias sphere, assign an importance of $B = \min(1/\sin\theta_{min}, P_{max})$ and reject the photon if $B < RP_{max}$. The efficiency of this rejection method is about $(1 + 2/\pi \bullet \log P_{max}) / P_{max}$ or about 14% for P_{max}=20. The importance of this efficiency depends on the amount of work that will be done with each accepted photon, but for very large P_{max}, particularly if coupled with the surface source rejection method, a search for a more efficient algorithm may be warranted.

IV. Test problems

A series of test problems have been run to 1) prove that these angular biasing techniques do not affect any physical results, 2) confirm the reduction in statistical noise and 3) determine the optimal value for P_{max}, the upper limit on polar biasing. The geometry is a spherical annulus of vacuum with inner radius R_0=0.35 which is used to tally and remove any photons striking it and an outer radius of 1.0 from which a source launches photons in a cosine distribution relative to the local surface normal. The spherical annulus is represented by K=20 equal angular zones in 90 degrees and the distribution of source intensity on the outer radius is $P_0 + 0.1\ P_2$, where P_L represents the L'th Legendre moment. One million photons were used in each simulation. The exact analytic result for the intensity distribution on the inner radius is $P_0 + 0.055062\ P_2$ (Haan,1994).

Table 1. Concentric sphere biasing test problems

	No biasing	Bias uniform toward sphere	Polar biasing, P_{max}=20
P_0	.995(.003)	.999(.001)	.997(.001)
P_2	.057(.006)	.057(.002)	.054(.003)
P_4	.009(.009)	.001(.003)	.003(.004)
P_6	.001(.010)	.003(.004)	.003(.004)
P_8	.022(.012)	.002(.004)	.002(.005)
N eq.	9555	71328	58951
N pole	444	3172	20156
Δf/f eq.	.0102	.0038	.0053
Δf/f pole	.0475	.0179	.0072

In Table 1 we list the Legendre moment expansion of the flux striking the inner radius with standard deviations given in parenthesis. Also given are the number of photons striking the equator and pole zones on the inner radius and the relative error in the flux at those zones. We see that all of the test problems give the analytic result of $P_0 + 0.055062\ P_2$ to within their statistical errors. Because of the cosine surface source emission the fraction of energy striking the inner radius is $1/R_0^2$, or 0.1225 for R_0=0.35. For isotropic emission it would be a factor of 4 smaller. Indeed, for the unbiased run about 12% of the one million photons did strike the inner radius, while virtually all photons struck the inner radius in the biased cases. A simple estimate of the expected standard deviations is $\sqrt{(2L + 1)/N}$, where L is the moment number and N is the number of (assumed equal weight) photons striking the inner radius. This fits the data in Table 1 quite accurately, although the polar biased case has somewhat larger errors due to the use of photon weights that vary by a factor of P_{max}. Polar biasing does not help reduce the variance in the moment expansion of the flux.

Turning our attention to equator and pole zonal tallies we see that for the non-polar biased cases the number of photons striking these zones is simply related to

their fractional area, $\pi/2K = 0.0785$ for the equator and $0.5(\pi/2K)^2 = 0.0031$ for the pole, and that the relative errors are precisely given by $1/\sqrt{n}$, where n is the number of photons striking the zone. For the polar biased case we see that the number of photons striking these two zones are more equal and that the error at the pole has been improved at the expense of the error at the equator. At the equator the error is larger than $1/\sqrt{n}$ because of the variation in the weights of the photons. Of course, for this test problem one could have used a polar biasing scheme that assumed a hard sphere and assigned photon weights according to the latitude of intersection with the bias sphere. This would have resulted in equal number of photons striking the equator and pole zone and the relative error in each would have been $\sqrt{K/N} = 0.0045$. Such a scheme was not implemented because it did not appear to be robust enough for real problems.

Table 2. Determination of optimal P_{max} for K=20

P_{max}	$\Delta f/f_{pole}$	cpu time (sec)	FOM
1	.0179	585	.187
2	.0154	669	.159
5	.0113	738	.094
10	.0089	796	.063
15	.0076	883	.051
20	.0072	934	.048
25	.0070	1018	.050
30	.0069	1078	.051
40	.0069	1165	.055
50	.0070	1312	.064
60	.0070	1431	.070
100	.0073	1862	.099

This leaves us with the problem of determining the optimal value for P_{max}. We have run a series of calculations with K=20 varying P_{max} from 1 to 100 and compared the relative polar error, $\Delta f/f$, in Table 2. Also given are the cpu times (sec) and an overall figure of merit (FOM) of $\text{cpu} \cdot (\Delta f/f)^2$. The cpu times increase with P_{max} because of the rejection algorithm used in establishing the photon directions. The relative polar error minimizes for $30 < P_{max} < 40$, but is very flat for $P_{max} > 20$ where the FOM is optimal. Although the FOM from this test problem series is not directly applicable to other problems where a different amount of work may be done with each accepted photon, the fact that optimal FOM occurs near the smallest P_{max} that achieves most of the reduction in $\Delta f/f$ is reason enough to choose $P_{max}=20$ as the optimal value. Although such a detailed study has not been carried out for different values of K it is anticipated that $P_{max}=K$ is always near optimal.

V. Discussion and summary

We have not yet discussed the optimal choice for $B(\mu)$, the importance of photons as a function of their cosine relative to the bias sphere center. In the test problem we simply made $B(\mu)$ large for all μ that would intersect the inner sphere, but in real hohlraum problems it will be necessary to use some photons to calculate the evolution of the hohlraum walls. The optimal choice is problem dependent, but it seems clear that using half of the total number of photons for the capsule and half for the hohlraum walls cannot be more than a factor of two away from the optimum. This can be accomplished by setting $B(\mu)=4\pi/\Delta\Omega$ for all μ that would intersect the capsule, where $\Delta\Omega$ is the solid angle of the capsule as seen from the wall. The overall effective gain in computing power due to angular biasing then is half this value times the gain from polar biasing, or

$$\frac{2\pi}{\Delta\Omega} \cdot \frac{K}{1 + 2/\pi \cdot \log K}$$ if we ignore the rejection costs.

For a capsule radius of 0.35 times the hohlraum radius and K=20 angular zones in 90 degrees this gain is greater than 100. We expect that 50 can be achieved in real problems.

References

Fleck, J. A., Jr. and Cummings, J. D., "An Implicit Monte Carlo Scheme for Calculating Time and Frequency Dependent Nonlinear Radiation Transport", *J. Comput. Phys.*, 8, 313-342 (1971).

Haan, S. W., *Radiation Transport Between Concentric Spheres*, Lawrence Livermore National Laboratory, Livermore, CA, UCRL-ID-118152 (1994).

Work performed under the auspices of the U. S. DOE by LLNL under contract no. W-7405-Eng-48.